X-ray PTV Measurements of Solitary Waves

L. Smith[1*], B. Hu[1, 2], J. Kolaas[1], A. Jensen[1] K. Sveen[1, 3]
1: Dept. of Mathematics, University of Oslo, Norway
2: Flow Capture, Norway
3: Institute for Energy Technology, Norway

* Correspondent author: lisasmi@math.uio.no

Keywords: X-ray measurements, 3D PTV, Solitary Waves

ABSTRACT

The aim of this study is to measure velocity fields and accurate surface elevation in solitary waves utilizing a fast X-ray PTV system. It is difficult to measure the free surface of water waves with the optical measurement techniques available today. This is partly due to refraction and reflection of light rays by the surface of the waves, or by reflections of light rays by the wall of the wave tank. The interface between water and air will then get an inaccurate location in images captured by visual light. The use of microelectronics in image sensors, have made it possible to capture images with both high spatial and temporal resolution. In this study, X-ray measurements with high resolution in space and time have been performed on solitary waves. Two perpendicular X-ray systems are utilized. Surface elevation measurements with accuracy of 0.12 mm are presented, and cross-waves due to wall effects are observed when the average wave height is subtracted from the images. Particles that absorb X-ray are seeded into the water and PTV is used to find velocities in the flow field. The two X-ray systems provided enough information to produce a 3D reconstruction of the flow field. The velocities measured are compared to velocities computed by a Boundary Integral Model (BIM). There seems to be discrepancy between the computed and the measured velocities, which may be linked to inaccuracy in the particle's location or linked to the large size of the particles.

1. Introduction

Wilhelm Röntgen was the first to generate and detect X-ray radiation (Stanton, 1896). X-rays have mostly been used in medical contexts, and an overview of *in vivo* measurements can be found in Fouras et al. (2009). In the recent work, X-ray measurements have been frequently used in experimental fluid mechanics. Several X-ray measurements have been performed to visualize multiphase pipe flow (see Vinegar and Wellington (1987) and Bin Hu et al. (2005)). One of the latest developments is to apply known image techniques such as Particle Tracking Velocimetry (PTV) to images captured with X-rays (Kertzscher, 2004). In X-ray PTV studies, the fluid must be seeded with X-ray absorbing particles, which also should be neutrally buoyant with respect to the fluid, as in regular PTV. Drake et al. (2011) have given a description on how these particles can be made.

Solitary waves were first observed by John Scott Russell in 1834 (Miles,1980). Typical solitary waves consist of one single crest and travel with constant speed without changing shape. They are nonlinear and dispersive waves. A full potential solution for solitary waves was found by Tanaka (1986), while Fenton (1972) found a ninth order approximative solution for solitary waves.

Until now, very few X-ray studies with high temporal and spatial resolution have been utilized in the field of experimental fluid mechanics. The purpose of this study is to measure surface elevation and 3D velocities of solitary waves, utilizing a fast X-ray system. Solitary waves are attractive to work with experimentally, since solitary waves can be easily generated in a wave tank, and the measurements can be validated against well-established solitary wave theory.

2. Experimental set-up

A sketch of the experimental set-up is shown in Figure 1. Solitary waves are generated in a 10 cm wide and 300 cm long wave tank made of Poly(methyl methacrylate), PMMA. The tank is mounted into an X-ray cabinet. Three different water depths are investigated ($H = 2.77, 2.92\ and\ 4.85\ cm$). Two X-ray sources are perpendicularly mounted on top and at the side of the wave tank. The X-ray radiation is distributed around a peak energy, which is set to 40 kV and 60 kV for the source mounted on top and the source from the side, respectively. The associated X-ray currents are set to 4.0 mA and 5.0 mA respectively. Two high-speed X-ray CMOS detectors are located on the opposite side of the X-ray sources. The detectors sensitive area is $114.9\ mm \times 64.6\ mm$ distributed by 1536×864 pixels. A multi-channel trigger source synchronizes the two detectors, and images are captured at 100 frames per second (fps) with an exposure time of $10ms$ and a 2×2 pixel binning. A block releasing wave maker generates solitary waves with three normalized amplitudes A/H (i.e. 0.48, 0.35 and 0.18), which are associated with the different water depths mentioned above. The wave maker and the X-ray system are positioned 6.5 and 200.5 cm from the inner left wall of the wave tank. Two acoustic wave gauges (ultra Banner U-Gage S18U), positioned at -13.74 and 6.26 cm from the middle plane of the X-ray systems, are used to measure the surface elevation.

The water is seeded with cylindrical X-ray absorbing particles with a varying length of $1 - 2\ mm$ and a diameter of 1 mm. The particles are made of foamy polymer with $(4 - 5)\%$ by volume metal (lead and/or tungsten). The average particle density is $1.04 \cdot 10^3\ kg/m^3$ with standard deviation 0.9 kg/m^3. The Stokes number for the particles varies from $0.8201 - 1.0851$ depending on the water depth. Even though the particle´s average density is designed to match

the water density, the slight density difference can still result in a large amount of the particles sinking rapidly to the bottom of the wave tank or floating to water surface. To improve the number of particles within the investigation area, a careful selection of particles has been performed by discarding the particles that drifted to the surface, and those that sank to the bottom.

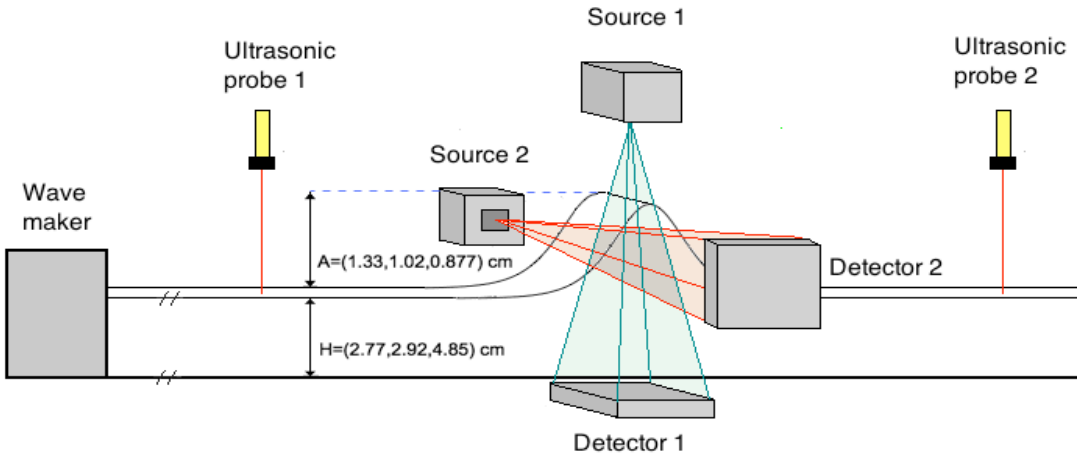

Figure 1: Experimental setup.

3. Post processing and PTV analysis.

To find accurate surface elevations, a large calibration data set of different water depth was collected. A logarithmic calibration curve was used for the top view while a second order polynomial curve was fitted to the side view data. The side view interphase was determined by the maximum vertical gradient of the images. Dropouts in the ultrasonic probe measurements, which occurred at steep regions, have been filled in by linear interpolation of proximity signals. In addition, cubic polynomial regression has been used to remove high-frequency noise from the ultrasonic signal.

To obtain three-dimensional velocities of the X-ray particle, a coupling of the measurements from the two X-ray cameras needs to be performed. Compared to the images obtained from the vertical measurements, the images captured from the side measurement have given much lower contrast between water and X-ray particles. This is as expected because the relative fraction of X-ray absorbed by seeding particles becomes smaller as the water depth increases. To enhance the contrast in the side images special image processing techniques have been applied:

- Background removal (Subtraction of an averaged still water image)
- Normalization

- Histogram equalizer
- Mask out the interphase (The interphase is found by the maximum vertical gradient.)

This has clearly enhanced the contrast between the background and the particles, but the boundaries of the particles will be affected by this procedure and the accuracy in the center location of the particles may be reduced. For the top view, the higher contrast allows for particle recognition by only performing the background removal and normalization processes.

Determination of the particles centers and velocities are performed in *DigiFlow* developed by Dalziel (2006). 3D-reconstruction of the positions is simply performed by basic geometry analysis, and by coupling the depicted particles captured by the two different cameras. This is fairly easy since the number of particles is relative limited (~8) and since the algorithm only matches particles based on their locations. Only particles that show a coinciding trajectory motion of their 3D positions with an error less than 0.15cm are considered.

To verify the velocity obtained by the X-ray system, the simulated values from the boundary Integral Model (BIM) were used for comparison. The BIM solver is essentially an inviscid potential flow model that computes the velocity field and surface elevation of solitary waves. More information on the BIM model can be found in Pedersen et al. (2013).

4. Results

The results are presented in two parts in this section. Firstly, the surface elevation measurements are presented, followed by the observations from the velocity measurement. Raw images of top and side views captured by the X-ray cameras from the experiments are shown in Figure 2. As shown by the side view (right image of Figure 2), the contrast between water and particles is low.

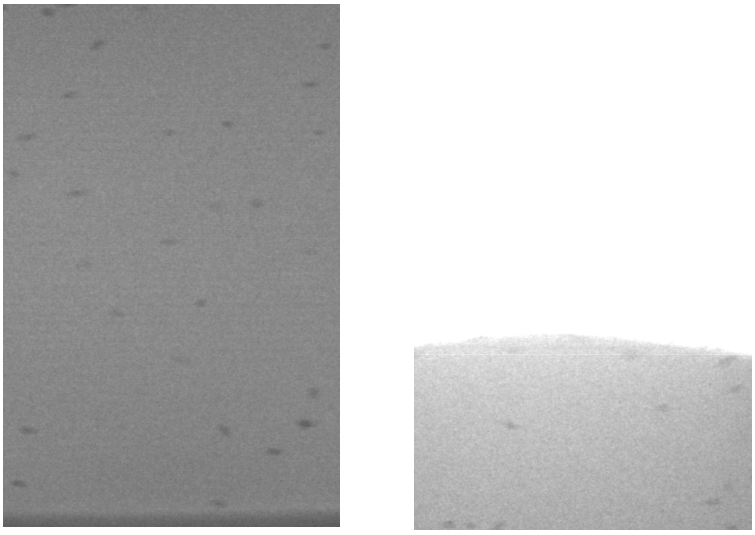

Figure 2: Raw images of the wave crest. Left: Top view Right: Side view.

4.1 Accurate surface elevation measurements

The surface elevation measured by X-rays, compared with the ultrasonic probe measurement, is shown in Figure 3 for the water depth (H) of 4.85 cm. The comparison has shown a very good

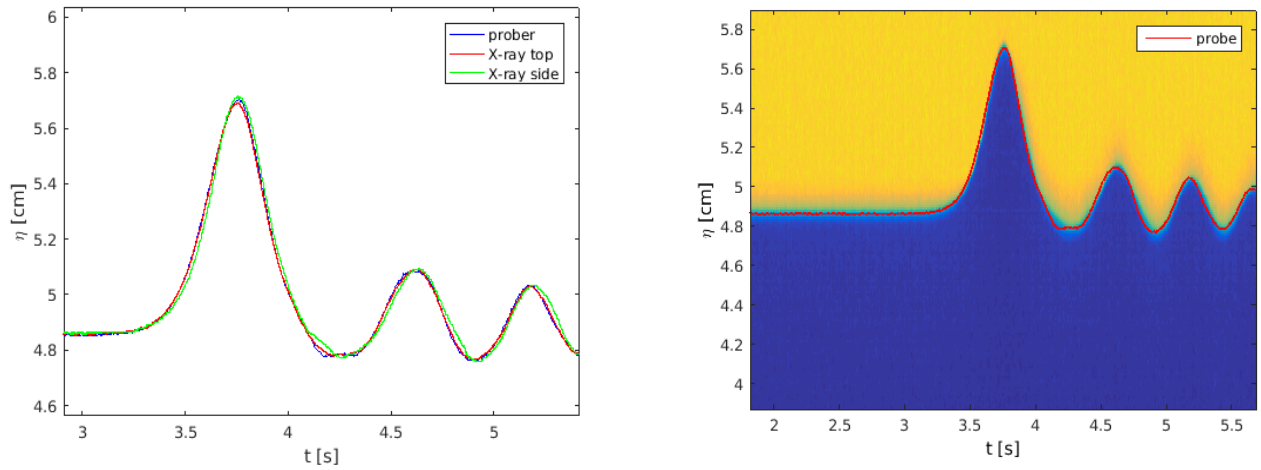

Figure 3: Surface elevation measured with X-ray and the ultra sonic probes. Left: Averaged top view and interphase from the side view. Right: Side view and probes.

agreement on the measured surface elevation between the ultrasonic and X-rays from both the side and top views. The X-ray measurements from the top and the side are smoothed with a first order Savitzky-Golay filter with a frame size of 0.028 s. The maximum deviation between the ultrasonic probe and the X-ray measurements is 0.12 mm for the top view, and 0.14 mm for the side view. This is prominent compared to the accuracy one can retrieve from the optical measurement techniques available today. The smaller waves captured after the large solitary wave are the reflected waves from the end walls of the wave tank.

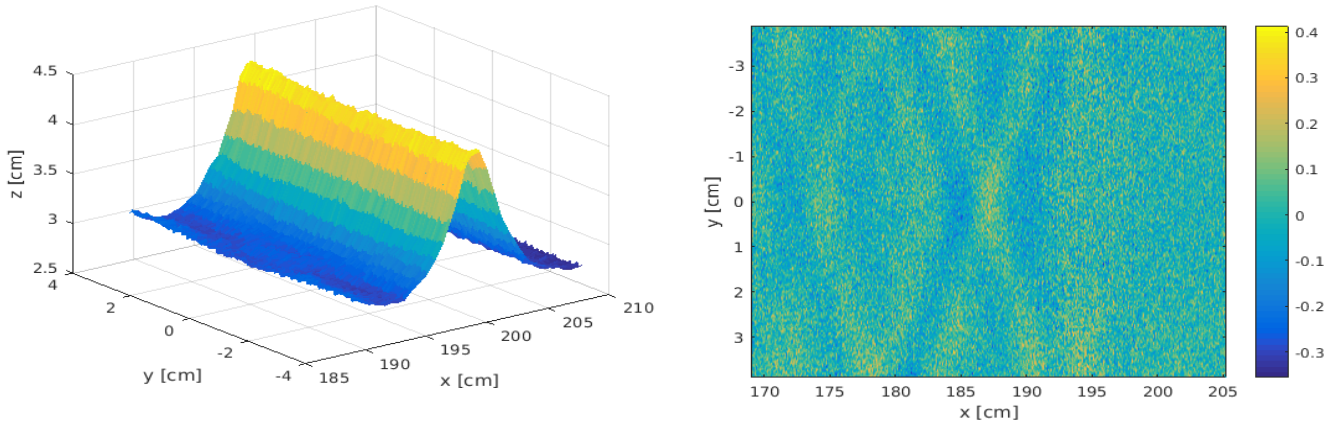

Figure 4: Left: 3D Spatial surface elevation, Right: Cross-waves obtained after the wave crest. Colour scale, [cm]

A 3D spatial resolved view of the waves is presented in Figure 4. The left figure shows the 3D surface elevation, reconstructed by correlating the surfaces from the image series. The right figure shows the deviation in the surface elevation in the cross section of the wave tank. The average surface elevation is subtracted from the original image and a smoothing filter is applied. The filter size was set to 50 × 5 pixels. After the solitary wave crest passes, a small cross-wave is observed. This is probably caused by wall effect from the wave tank.

4.2 Measured velocities

Figure 5 shows 3D trajectories of the X-ray particles collected from four different runs from the experiment with the water depth (H) of 2.77 cm. The coordinate origin is set to the middle of the detectors for (x, y), and at bottom of the wave tank. $t = 0$ correspond to the time when the wave crest is centered in the images. Although great effort has been made to increase the number of particles within the investigation area, the number of particles is still not as large as one would normally require for accurate quantitative analysis. The background shows the measured surface elevation.

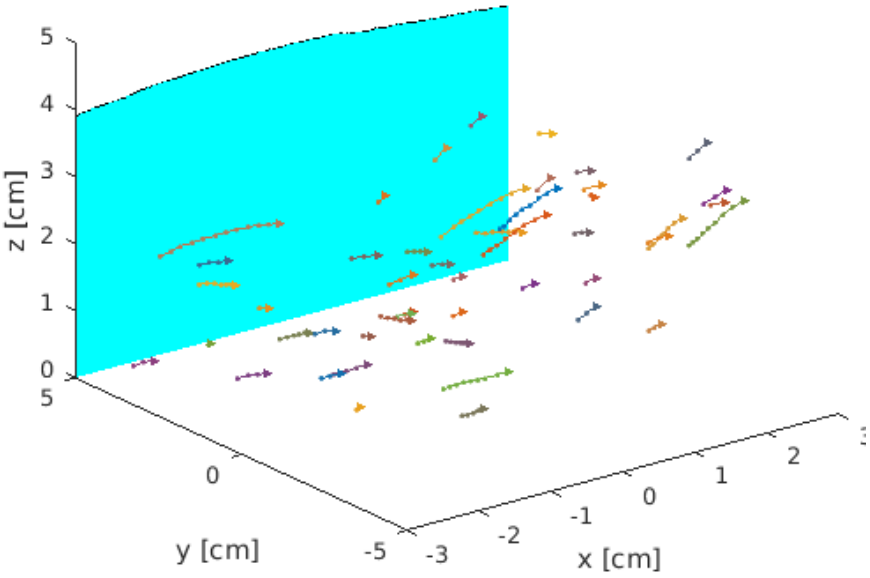

Figure 5: 3D trajectories of particles collected from $-\mathbf{0.10s} < \mathbf{t} < \mathbf{0.10s}$. t=0 corresponds to the time when the solitary wave crest is captured in the centre of the detectors.

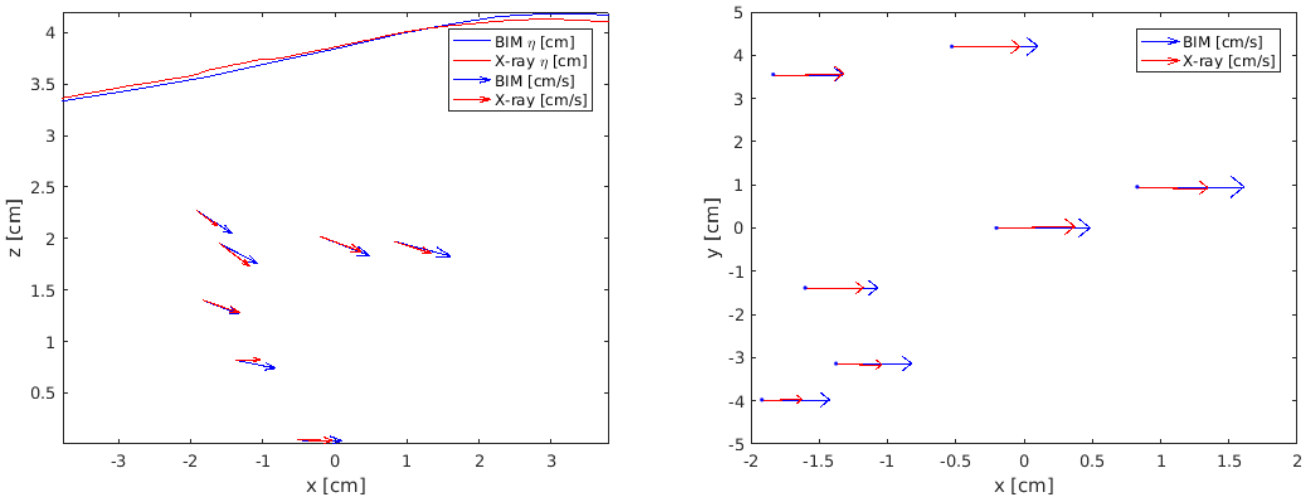

Figure 6: Velocities at t=0.04s, Left: Side view, the solid lines marks the surface, Right: Top view

Figure 6 shows the measured velocities of the X-ray particles in comparison with the velocities computed by the BIM solver. In general, there is a fairly good agreement between the simulation and experiments. Nevertheless, slight discrepancies from BIM are observed for the measured velocities. The average velocity magnitude difference is 23 % for the particles obtained at $t = 0.04\ s$. The discrepancies may be due to the relative high stokes number calculated for the particles. The particles may not follow the flow fidelity, and inertia forces might affect the particles. The image processing performed on the images from the side, will introduce a small error in the center location of the particles, and this may be one of the reasons for the deviations in Figure 6.

5. Conclusion

In the present study, X-ray measurements of solitary waves were investigated in a small-scale wave tank facility. Accurate surface elevation measurements were conducted with an accuracy of 0.12 mm. A cross-wave was observed behind the solitary wave crest, and is most likely caused by wall effects from the wave tank.

3D velocity measurements of X-ray particles were investigated and compared with computed velocities from numerical simulations. There were some discrepancies between the computed and the measured velocities, which were linked to the X-ray particles stokes number, and the uncertainties related to the particles location in the images. A smaller wave tank will enhance the contrast between the water and the particles in the images from the side, and this may improve the accuracy in the particles location. The particles used in the current experiment

are not optimal for this setup, and it would be beneficial to use smaller particles with a less wide and more similar to water density distribution.

Finally as indicated in the present study, the fast X-ray system is an excellent measurement technique for obtaining accurate interfaces and flow characteristics associated with solitary waves. In particular, it brings a superior feature when 3D spatial velocities fields are desired.

Acknowledgement

This work was funded by the Research Council of Norway through the research project DOMT - Developments in Optical Measurement Technologies (project number 231491).

References

- Dalziel, S. B., 2006. Digiflow user guide. http://www.damtp.cam.ac.uk/lab/digiflow/digiflow.pdf, [On- line; accessed 20-Aug-2014].
- Drake, J. B., Kenney, A. L., Morgan, T. B. and Heindel, T. J. (2011), Developing tracer particles for x-ray particle tracking velocimetry, in 'ASME- JSME-KSME 2011 Joint Fluids Engineering Conference', American Society of Mechanical Engineers, pp. 2685–2692.
- Fenton, J. (1972), "A ninth-order solution for the solitary wave", Journal of fluid mechanics, Vol. 53, Cambridge Univ Press, pp. 257–271.
- Fouras, A., Kitchen, M., Dubsky, S., Lewis, R., Hooper, S. and Hourigan, K. (2009), "The past, present, and future of x-ray technology for in vivo imaging of function and form", Journal of Applied Physics, Vol. 105, AIP Publishing, p. 102009.
- Hu, B., Stewart, C., Hale, C. P., Lawrence, C. J., Hall, A. R., Zwiens, H. and Hewitt, G. F. (2005), "Development of an x-ray computed tomography (ct) system with sparse sources: application to three-phase pipe flow visualization", Experiments in fluids, Vol. 39, Springer, pp. 667–678.
- Kertzscher, U., Seeger, A., Affeld, K., Goubergrits, L. and Wellnhofer, E. (2004), "X-ray based particle tracking velocimetry -a measurement technique for multi-phase flows and flows without optical access", Flow Measurement and Instrumentation, Vol. 15, Elsevier, pp. 199–206.
- Miles, J. W. (1980), "Solitary waves", Annual review of fluid mechanics, Vol. 12, Annual Reviews 4139 El Camino Way, PO Box 10139, Palo Alto, CA 94303-0139, USA, pp. 11–43.

- Pedersen, G., Lindstrøm, E., Bertelsen, A., Jensen, A., Laskovski, D., Sælevik, G., 2013. Runup and boundary layers on sloping beaches. Physics of Fluids (1994-present) 25 (1), 012102.
- Stanton, A. (1896), "Wilhelm Conrad Rnöntgen on a new kind of rays: translation of a paper read before the würzburg physical and medical society, 1895", Nature, Vol. 53, pp. 274–276.
- Tanaka, M. (1986), "The stability of solitary waves", Physics of Fluids (1958- 1988), Vol. 29, AIP Publishing, pp. 650–655.
- Vinegar, H. J. and Wellington, S. L. (1987), "Tomographic imaging of three- phase flow experiments", Review of Scientific Instruments, Vol. 58, AIP Publishing, pp. 96–107.